ResearchGate

See discussions, stats, and author profiles for this publication at: https://www.researchgate.net/publication/226460014

Structural control of a masonry vault

Article *in* Structural and Multidisciplinary Optimization · November 2002

DOI: 10.1007/s00158-002-0250-y

CITATIONS
0

READS
46

3 authors, including:

Maurizio Brocato
Ecole Nationale Supérieure D'Architecture Paris-Malaquais, France

58 PUBLICATIONS **136** CITATIONS

SEE PROFILE

Some of the authors of this publication are also working on these related projects:

Project

International Symposium on "micro to MACRO mathematical modelling in soil mechanics" View project

All content following this page was uploaded by Maurizio Brocato on 05 June 2014.

The user has requested enhancement of the downloaded file.

Struct Multidisc Optim 24, 387–395 © Springer-Verlag 2002
Digital Object Identifier (DOI) 10.1007/s00158-002-0250-y

Structural control of a masonry vault

M. Brocato, A. De Domenico and F. Zanghì

Abstract Ancient buildings sometimes need to be supplied with reinforcing structures. Active reinforcements can be the right answer to quite complex, and widely unknown working conditions. Their design requires, in particular, the choice of a control policy and the optimal design of sensors-processors-actuators.

The vault of the *Maggior Consiglio* Hall in the Duke's Palace of Genoa, although presently supported by an auxiliary truss, undergoes relatively large displacements, probably due to temperature variations; the use of stiffer links to reduce these displacements may result into high thermal stresses. This problem is studied here as an example of the design of a control system.

A numerical model of the structure is proposed, and a performance function is considered; a feedback loop is designed and the corresponding algorithm is given. The inverse problem of determining the actuating forces following variable external condition to achieve the best performance is solved. Results show the feasibility of the method.

Key words brick masonry, intelligent structures, reinforcement, structural control

1 Foreword

The structural rehabilitation of heritage masonry buildings often demands the introduction of auxiliary structures the compatibility of which becomes then a major problem. For instance the linkage between the old and the new fabric must be designed to avoid unwanted constraints, stress concentrations which would localize damage, etc.

Controlled auxiliary structures [as often proposed for seismic hazard mitigation; SCR Panel (1997)] will probably require growing attention in the future. They can answer the need of ready adaptation to predictable, but poorly determinable, events, supplying the old structure with energy dissipation capacity (e.g. through passive or semi-active devices) or control forces (active systems) where and when needed. For instance active linkage systems between old and new timbers can provide the sufficient strength with the necessary flexibility or ductility in view of partly indeterminate load conditions.

The use of active devices requires the definition of a control policy and the design of a control system fit to implement the strategy. Information to generate appropriate control actions can be obtained monitoring the input load (feedforward control) and/or the output response of the structure (feedback). Feedforward algorithms may be hindered, in practice, due to the relatively poor quality of estimation of available mathematical models of complex masonry structures and to the lack of data on the interweaving and constitution of materials within foundations, walls, vaults, etc. Consequently, as in most engineering applications, feedback generated controls are most probably needed.

It is to be expected, in general, that ancient structures behave nonlinearly, especially if, as in seismic circumstances, their strength resources must eventually be wholly exploited. A proficient mathematical model of the structure must then anyway be included in the control system, in order to predict the effects of application of the feedback generated control actions. These actions must then be constrained to avoid damaging the ancient structure, so that, again, a reliable predictive model is paramount. Due to the constraint, the controllability of the system must be checked.

2 Introduction

The vault of the *Maggior Consiglio* Hall in the Duke's Palace of Genoa was built shortly after a fire destroyed

Received October 25, 2001

M. Brocato, A. De Domenico and F. Zanghì

IEI-CNR, Area della Ricerca di Pisa, 1, via G. Moruzzi, 56124 Pisa, Italy and
LAMI-ENPC/LCPC, 6 et 8, avenue B. Pascal, Cité Descartes, Champs sur Marne, 77455 Marne la Vallée Cedex, France
e-mail: brocato@iei.pi.cnr.it
a.dedomenico@iei.pi.cnr.it
f.zanghi@iei.pi.cnr.it

the first floor of the Palace in 1777. To reduce the vulnerability to future events of the kind, Simone Cantoni, the architect, conceived an entirely masonry structure to cover the $17\,\mathrm{m} \times 35\,\mathrm{m}$ surface of the greater hall of the palace; due to the wide span and, probably, to the desired appearance, two superposed vaults, a ceiling and a roof, were built.

Due to some structural problem (perhaps a settlement of the foundation or of the underlying medieval structure, or some kind of technical error), occurring already during building in 1783, the vaulted ceiling underwent localized distortions. The thrust of the arches of the outer vault on the wall of the southern facade of the palace was then partly reduced by four tie rods.

Presuming this thrust to be the main cause of the disease, the heavy masonry covering was removed in 1861 by architect Ignazio Gardella, and a roof supported by iron trusses was built in its place. Each of the four damaged arches of the remaining inner vault, now under risk of local failure, was tied with rods to the truss above. Also the facade was reinforced with buttresses formed into two orders of columns. Improvements notwithstanding, the degradation of the vault did not stop.

During the last restoration of the palace, ending in 1992, steps were taken to reduce or eliminate the structural weakness of the vault. The walls supporting it were supplied with a concrete ring-beam at the level of the eaves and were reinforced through injections and micropiles; auxiliary iron truss-beams were built between the vault and the roof and they were connected to the vault to support it through a number of springs (Croci 1986; Osti *et al.* 1988).

Although the risk of failure is presently reasonably reduced, movements of the vault can still be observed and seem to cause damage, at least to the ornaments and frescoes of the magnificent ceiling. A measurement campaign carried out by the authors of the restoration project in 1992 shows that a close correlation exists between these movements and the external temperature. Obviously, mainly vertical displacements result from thermal dilatations of the vault due to its lateral confinement. This lateral confinement, needed for convenient structural answers to the vault's thrust, plays a fundamental role in the amplification of the vertical component of the thermal displacements. The irregular curvature of the vault causes then strain concentration and, possibly, localized damage.

Although only slow phenomena are involved, the cyclic nature of the thermal load must be considered as particularly critical for the masonry structure. Some of the mortar joints in the most stressed regions of the structure may undergo cycles of opening/closing of microcracks (and even of macroscopic fractures) to accomplish the overall deformation. In these conditions the stability of cracks propagation need be verified.

To reduce the risk of increasing damage one should wish to confine the amplitude of cyclic displacements due to the thermal load. With a standard, passive, reinforcement, the only possible way to achieve this result is to constrain even further the displacements, e.g. linking the vault to the auxiliary structure with stiffer springs or even through very rigid rods. A drawback of this strategy (which was certainly discarded by the authors of the restoration project) is that it increases the thermal stresses and eventually creates more problems than it solves.

A smarter approach would be to replace the springs currently linking the auxiliary structure to the vault with motion or force controllers (electrohydraulic or electromechanical, hard or soft devices) and implement an appropriate control strategy of the system. The target could be a minimum deviation of the displacement of the vault from some ideal conditions (say, the static deflections under permanent load at uniform temperature, the latter being chosen, e.g. as the mean temperature in the season).

We study the feasibility of a feedback control on the vault under external thermal cyclic loads using active soft bonds to link the vault and the truss.

In the first part of the paper we present a FEM model of the vault, including the auxiliary structure and the actuators; attention is paid to the boundary conditions for the structure and to the mathematical model of the masonry vault and walls. The computational model which we present here is supposed to be part of an active control code, therefore it must satisfy requirements of minimal size.

In the second part of the paper we define a control strategy, which calls upon the active tendons between the vault and the truss to slow down the damage of the decorations. A feedback control on the vault under external thermal cyclic loads is studied. The output measures needed to feed the control loop are obtained through the FEM model of the vault, taking a simulated temperature variations from the coldest to the hottest possible conditions for the site (extreme winter and summer conditions). The same model is used to evaluate, at each step of loading, the correlation matrix governing the control.

Our results show the feasibility of the control. The overall displacement of the vault can be reduced to up to half its present value, in both winter and summer extreme thermal load conditions, with a reduction, in the mean time, of the maximum stresses: the control distributes more evenly the elastic deformation of the vault, avoiding stress concentrations that are presently responsible for the degradation of the structure or, at least, of the coating.

3 Computational model

3.1 Description of the structure

The masonry structure of the vault was conceived as a suite of six parallel curved ribs, leaning on the longer walls of the rectangular hall; two central couples of ribs

divide the covered surface into three almost equal areas; rampant arch ribs, abutting on the shorter walls of the hall, radiate from the first and last rib of the above-mentioned suite; masonry foils cover the span between ribs.

Each of the two central couples of main ribs has undergone a large deformation on the side next to the facade. As the foils in between followed their movement, two large bumps appear on the vault.

The auxiliary structure built between the vault and the roof is made of iron truss-beams, one above each rib of the masonry structure. These beams are supported through pinned ends by plates at the top of a concrete ring-beam placed at the eaves, with micro-piles reinforcing the ancient masonry walls below the ring-beam.

We assume that ten force actuator devices (such as hydraulic cylinders) can be mounted linking the vault and the auxiliary structure (on the same pins presently supporting the springs). The corresponding structural element in the model is that of pre-stressed bar (with assigned, relatively low, stiffness). The prestress is assumed to be assigned at will, between the limits of safety of the linkage presently installed on the vault.

Our scope is the definition of a numerical model of the structure described above, which will be used for on-line calculations at each step of a control algorithm. To fit the computational effort with the requirement of a prompt reaction of the control, we choose to model the structure as a two dimensional system laying on a vault's cross-sectional plane, undergoing small displacements and small strains. The model includes a single main rib of the vault, with portions of the foils next to it, the truss-beam above the rib, and the walls supporting the rib from the floor of the hall to the eaves. The nineteenth century roof and trusses are considered as dead vertical loads on the eaves. Fictitious elements are added to represent roughly the concrete ring-beam, the column buttresses of the facade, the medieval structures below the hall and the adjacent vaults of the *Minor Consiglio* Hall.

3.2 Constitutive model

The masonry structure of the vault's rib is compound of brick courses and mortar beds approximately laying on radial planes. Such anisotropic constitution is crucial, as it favours the displacements of the vault along the radial direction.

The constitutive model of masonry considered here is that of an orthotropic linear elastic material, with the symmetry axis normal to the plane of the layers. This plane is horizontal within walls and radial in the vault.

The choice of excluding irreversible effects (e.g. damage or fracture) is related to our particular scope: to guarantee a longer life to the structure a proper control strategy should, in principle, avoid the occurrence of irreversible phenomena.

For a brief description of the homogeneous orthotropic model we use Speciale *et al.* (2001). Let us consider a body compound of thin and thick layers of mortar and bricks respectively, with index A referring to bricks and B to mortar; let λ and μ denote Lame's coefficients as usual, η_A, η_B the volume fractions of constituents ($\eta_A + \eta_B = 1$). The model is based on the assumption of uniform stress within the thin mortar layers and of perfect contact between mortar and bricks.

Within the limits of a Voigt approximation of the overall behaviour of the layered material (uniform deformation), the compliance tensor is

$$\mathbf{S}_H = (1-\eta_B)\,\mathbf{S}_A + \eta_B \mathbf{S}^* \,, \tag{1}$$

where

$$\mathbf{S}_A = \frac{1}{2\mu_A}\mathbf{I} - \frac{\lambda_A}{2\mu_A(2\mu_A+3\lambda_A)} I \otimes I \tag{2}$$

(I and $\mathbf{I}$ being, respectively, the second and fourth order identity tensors) and

$$S^*_{1111} = S^*_{2222} = S^*_{1122} = \frac{\mu_B(2\mu_B+3\lambda_B)}{\phi^2} \,,$$

$$S^*_{1133} = S^*_{2233} = \frac{\mu_B(2\mu_B+3\lambda_B)}{\phi\varphi(2\mu_B+\lambda_B)} \,,$$

$$S^*_{3333} = \frac{\mu_B+\lambda_B}{\varphi^2} + \frac{2\lambda_B}{\varphi\vartheta} + \frac{2\mu_B+\lambda_B}{\vartheta^2} \,,$$

$$S^*_{1313} = S^*_{2323} = \frac{1}{2\mu_B} \,, \tag{3}$$

all other components of $\mathbf{S}^*$ being either given by symmetry or null, and where

$$\phi := \frac{2\mu_A(2\mu_A+3\lambda_A)\left(\lambda_B^2 - (\mu^*+\lambda^*)(\lambda_B+2\mu_B)\right)}{\lambda_A^2(\lambda_B+2\mu_B)} \,,$$

$$\varphi := \frac{\mu_A(2\mu_A+3\lambda_A)\left(\lambda_B^2 - (\mu^*+\lambda^*)(\lambda_B+2\mu_B)\right)}{\lambda_B\mu_A(2\mu_A+3\lambda_A) - \lambda_A(\mu_A+\lambda_A)(\lambda_B+2\mu_B)} \,,$$

$$\vartheta := \frac{\mu_A(2\mu_A+3\lambda_A)\left(\lambda_B^2 - (\mu^*+\lambda^*)(\lambda_B+2\mu_B)\right)}{\lambda_B\lambda_A(\mu_A+\lambda_A) - \mu_A(2\mu_A+3\lambda_A)(\mu^*+\lambda^*)} \,,$$

$$\lambda^* := \lambda_B - \lambda_B \,, \quad \mu^* = \mu_B - \mu_A \,, \tag{4}$$

The numerical results presented later in this paper have been obtained considering brick courses 12 cm thick, mortar beds 5 mm thick, and the following values for the elastic coefficients of the two materials: $\mu_A = 980$ MPa, $\lambda_A = 654$ MPa, $\mu_B = 29$ MPa, $\lambda_B = 0$ (i.e. Young's moduli and Poisson's ratios of the two materials are $E_A = 2.352$ GPa, $E_B = 0.060$ GPa, $\nu_A = 0.20$, $\nu_B = 0$).

The other material characteristics of masonry and steel which enter our computations are given below in Table 1.

Table 1 Material characteristics of masonry and steel

Masonry	
density	$2000\,\mathrm{kg\,m^{-3}}$
thermal expansion coeff.	$8\times10^{-6}\,{}^\circ\mathrm{C}^{-1}$
conductibility	$0.81\,\mathrm{J\,{}^\circ C^{-1}\,m}$
Steel	
Young's modulus	2.1×10^{2} GPa
Poisson's ratio	0.3
density	$7865\,\mathrm{kg\,m^{-3}}$
thermal expansion coeff.	$10\times10^{-6}\,{}^\circ\mathrm{C}^{-1}$

3.3 Structural model

The system under analysis is compound of the ancient masonry structure, the reinforcement given by the iron truss-beam and the concrete ring-beam, and the controllable force actuators in between the vault and the truss. Although these structures are actually embedded in a larger building, as already mentioned only a two-dimensional model of a part of the palace will be considered here.

The static sketch of the structure is given in Fig. 1; the structure is drawn with the side along the facade at the right-hand side of the picture. The parts of the palace below the floor level and on the left of the inner wall of the hall, which are not represented in the figures, will not be included in the analysis but through simplifying assumptions.

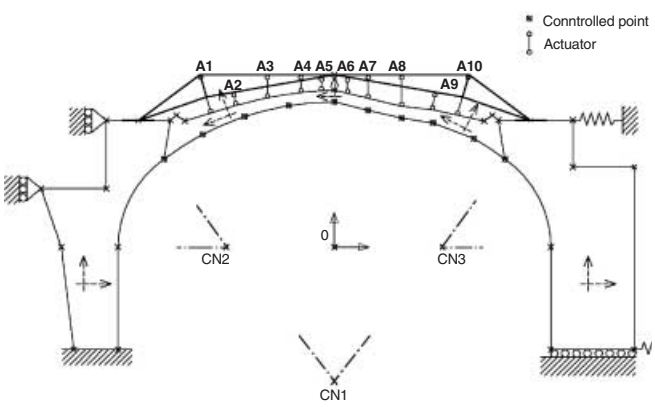

Fig. 1 Static sketch of the vault

The masonry structure is modelled as a planar domain, including the walls supporting the vault from the floor of the hall to the eaves and the vault itself. The domain is meshed into six-node triangular elements undergoing planar deformation; it is divided into five portions with different material parameters due to divers anisotropy directions, the axis of symmetry being vertical on the two side walls and radial along the curve of the vault (which, having three centres, requires three different portions to be modelled from the constitutive point of view).

The auxiliary truss structure is modelled as a framework of ten Euler-Bernoulli linear elastic homogeneous beams with seven nodes. The two structures are connected through force actuators and through the two pinned ends of the truss beam supported by plates; the latter are modelled as constraints to the rotational degrees of freedom of the nodes of the mesh of the masonry structure in contact with them.

The ten active tendons connecting the truss-beam and the walls are modelled as very compliant pre-stressed bar elements, the prestress being assigned through the control algorithm.

To take approximately into account the confinement effect produced, in the real three dimensional condition, by the concrete ring-beam, the horizontal translations of the eave on the left hand side of the figures is constrained to zero and that on the right hand side is linked with a spring, the stiffness coefficient of which is 1.857 MN/m.

All nodes on the boundary at the bottom of the inner (left-hand) wall are supposedly fixed; the lowest rank of nodes of the outer (right-hand) wall is totally constrained in the vertical direction while their horizontal displacements are related to a linear spring. The stiffness of this spring is 91.937 MN/m and is supposed to be approximately equivalent to the shear stiffness of the masonry walls and columns working as buttress below the floor level of the hall and not otherwise included in the finite element mesh.

After a separate computation, the roof is assumed to act on the two pins supporting its truss beam structure with equal vertical forces of 22.450 kN and with an horizontal thrust of 47.069 kN.

3.4 Thermal load conditions

The only variable loads, controllers apart, are the thermal loads induced by variations of the external temperature. We model these variations through a random fluctuation about the average seasonal temperature, which is considered to change from winter to summer given extreme conditions following a sinusoidal law. The extreme conditions are given in Table 2 (in °C).

Table 2 The extreme conditions

	W	S
indoor room temp.	15	20
room temp. between roof and vault	−5	40
outdoor temp.	−5	30

Note that the temperature under the roof is supposed to be higher than outdoors due to heat radiation on the dark grey tiles.

4 Control problem

4.1 Position of the problem

Call $\mathbf{u}$ the array of generalized displacements relative to the degrees of freedom of the whole structure, $\mathbf{K}$ the stiffness matrix, $\mathbf{f}$ the array of generalized forces acting on the structure. Consider a partition of the degrees of freedom, use index u to denote the degrees on which the controls act, x for the degrees which must be controlled, and s for all the others.

The stiffness matrix and the arrays of generalized forces and displacements can be partitioned as

$$\mathbf{K} = \begin{bmatrix} \mathbf{K}_{uu} & \mathbf{K}_{ux} & \mathbf{K}_{us} \\ \mathbf{K}_{ux}^T & \mathbf{K}_{xx} & \mathbf{K}_{xs} \\ \mathbf{K}_{us}^T & \mathbf{K}_{xs}^T & \mathbf{K}_{ss} \end{bmatrix} , \ \mathbf{f} = \begin{bmatrix} \mathbf{f}_u \\ \mathbf{f}_x \\ \mathbf{f}_s \end{bmatrix} , \ \mathbf{u} = \begin{bmatrix} \mathbf{u}_u \\ \mathbf{u}_x \\ \mathbf{u}_s \end{bmatrix} . \tag{5}$$

Let $\mathbf{f}^{(\theta)}$ be a particular thermal load condition, $\mathbf{f}^{(\gamma)}$ the permanent loads, and $\mathbf{f}_u^{(\kappa)}$ a particular set of forces applied on the structure by the actuators; by assumption it is $\mathbf{f}_x^{(\kappa)} = \mathbf{0}$ and $\mathbf{f}_s^{(\kappa)} = \mathbf{0}$. Similarly we denote by $\mathbf{u}^{(\theta)}$ the solution due to a particular temperature condition (other loads being excluded), $\mathbf{u}^{(\gamma)}$ the solution under permanent loads only, $\mathbf{u}^{(\kappa)}$ the solution under a given set of controls. To compact notations we will denote combined loads with the sum of exponents

$$\mathbf{f} = \mathbf{f}^{(\theta)} + \mathbf{f}^{(\gamma)} + \mathbf{f}^{(\kappa)} = \mathbf{f}^{(\theta+\gamma+\kappa)} ; \tag{6}$$

the same notation will be adopted for the displacements under combined loads in the linear case and, in any case, for the increments of displacement or force.

As already mentioned there are technical limits to the force that can be impressed on the structure through the actuators. Call $\overline{f}$ the absolute value of such a limit on a single linkage (here for shortness we assume all linkages working below a force of equal absolute value in the positive and negative directions); each control force must verify the conditions

$$-\overline{f} \le f_{ui} \le \overline{f} \quad \forall i , \tag{7}$$

where a_i denotes the i-th entry of the array $\mathbf{a}$ and clearly $\mathbf{f}_u = \mathbf{f}_u^{(\theta+\gamma+\kappa)}$ (notice that the actuators being relatively compliant, so as to give the effect of soft device, the first two contributions to the whole force ought to be significantly smaller than the third; $|f_{u_i}^{(\theta+\gamma)}| \ll |f_{u_i}^{(\kappa)}|$).

Temperature variations being rather slow, it is reasonable to assume that prompt control reactions will anyway be slow enough not to raise (undesirable) dynamic effects on the structure; then the description of the system can be done neglecting inertial forces. Furthermore, nonlinear effects, if any, are also assumed here to be time independent (e.g. quasi-static opening and closing of cracks, deformation induced damage, etc.).

4.2 Control algorithm

4.2.1 Linear optimal control

To discuss a simple strategy, let us first assume that "x" and "u" degrees of freedom coincide: one controls directly some of the generalized displacements. All others indirectly controlled degrees of freedom are marked with 's'. Denoting with the same indices the corresponding parts of the stiffness matrix,

$$\mathbf{K} = \begin{bmatrix} \mathbf{K}_{uu} & \mathbf{K}_{us} \\ \mathbf{K}_{us}^T & \mathbf{K}_{ss} \end{bmatrix} ; \tag{8}$$

let us call $\mathbf{H} = \mathbf{K}_{uu} - \mathbf{K}_{us}\mathbf{K}_{ss}^{-1}\mathbf{K}_{us}^T$; if the problem is linear we have the condensed system for the part of the solution depending on the control

$$\begin{cases} \mathbf{H}\mathbf{u}_u^{(\kappa)} = \mathbf{f}_u^{(\kappa)} , \\ \mathbf{u}_s^{(\kappa)} = -\mathbf{K}_{ss}^{-1}\mathbf{K}_{us}^T\mathbf{u}_u^{(\kappa)} . \end{cases} \tag{9}$$

A simple, direct strategy could be to impose, if possible, such prestresses that the controlled degrees of freedom remain in the position given by permanent loads at all time, which is implied by $\mathbf{u}_u^{(\kappa)} + \mathbf{u}_u^{(\theta)} = 0$, and keep the actuating force at its limit value if the prestress needed to achieve that result is larger than this value; i.e. the control law,

$$f_{u_i}^{(\kappa)} = \begin{cases} -H_{ij}u_{u_j}^{(\theta)} & \text{if } -\bar{f} \le f_{u_i}^{(\gamma+\theta)} - H_{ij}u_{u_j}^{(\theta)} \le \bar{f} , \\ \bar{f} & \text{if } f_{u_i}^{(\gamma+\theta)} - H_{ij}u_{u_j}^{(\theta)} \ge \bar{f} , \\ -\bar{f} & \text{if } -f_{u_i}^{(\gamma+\theta)} + H_{ij}u_{u_j}^{(\theta)} \ge \bar{f} . \end{cases} \tag{10}$$

The possibility of acting directly upon the degrees of freedom which need be controlled is seldom at hand in structural mechanics. When such direct control is infeasible or unfit, the linear optimal control law is slightly more complex; furthermore one may wish to have a performance index of the controlled degrees of freedom, e.g. a scalar function

$$\phi := (\mathbf{u}_x - \mathbf{w})^T\mathbf{W}(\mathbf{u}_x - \mathbf{w}) \tag{11}$$

to be minimized through a fit choice of $\mathbf{f}_u^{(\kappa)}$, $\mathbf{w}$ and $\mathbf{W}$ being chosen at will, depending on engineering requirements (e.g. $\mathbf{w}$ can be a given list of wanted offset generalized displacements of type x, and $\mathbf{W}$ can be a diagonal matrix with larger elements corresponding to the degrees of freedom one wishes to keep under a tighter control).

To shorten some of the following formulae, let us call

$$\begin{bmatrix}\mathbf{\Phi}_{xu}\\ \mathbf{\Phi}_{su}\end{bmatrix} = \begin{bmatrix}\mathbf{K}_{xx} & \mathbf{K}_{xs}\\ \mathbf{K}_{xs}^T & \mathbf{K}_{ss}\end{bmatrix}^{-1}\begin{bmatrix}\mathbf{K}_{ux}^T\\ \mathbf{K}_{us}^T\end{bmatrix},$$

$$\mathbf{C} = \mathbf{K}_{uu} - \begin{bmatrix}\mathbf{K}_{ux} & \mathbf{K}_{us}\end{bmatrix}\begin{bmatrix}\mathbf{\Phi}_{xu}\\ \mathbf{\Phi}_{su}\end{bmatrix}, \tag{12}$$

$$\mathbf{S}_{xu} = \mathbf{\Phi}_{xu}\mathbf{C}^{-1},$$

where $\mathbf{S}_{xu}$ denotes the correlation matrix giving generalized displacements of type x corresponding to unit forces of type u.

It is also useful to distinguish the solution control forces falling strictly within the admissible range,

$$\mathbf{f}_{\hat{u}}^{(\kappa)} \;:\quad |f_{\hat{u}i}| < \bar{f} \quad \forall i\,, \tag{13}$$

from those hitting the boundary of that range,

$$\mathbf{f}_{\bar{u}}^{(\kappa)} \;:\quad |f_{\bar{u}i}| = \bar{f} \quad \forall i\,. \tag{14}$$

A similar partition applies to $\mathbf{S}_{xu}$,

$$\mathbf{S}_{xu}\mathbf{f}_u^{(\kappa)} = \mathbf{S}_{x\hat{u}}\mathbf{f}_{\hat{u}}^{(\kappa)} + \mathbf{S}_{x\bar{u}}\mathbf{f}_{\bar{u}}^{(\kappa)}\,. \tag{15}$$

The constrained minimum to find for linear optimal remote control is

$$\min_{\mathbf{f}_u^{(\kappa)}}\left\{\phi\left(\mathbf{u}_x^{(\theta+\gamma)},\mathbf{f}_u^{(\kappa)}\right) \quad | \quad |f_{ui}| \le \bar{f}\;\forall i\right\}$$
$$\phi\left(\mathbf{u}_x^{(\theta+\gamma)},\mathbf{f}_u^{(\kappa)}\right) =$$
$$\left(\mathbf{S}_{xu}\mathbf{f}_u^{(\kappa)} + \mathbf{u}_x^{(\theta+\gamma)} - \mathbf{w}\right)^T \mathbf{W}\left(\mathbf{S}_{xu}\mathbf{f}_u^{(\kappa)} + \mathbf{u}_x^{(\theta+\gamma)} - \mathbf{w}\right)\,. \tag{16}$$

The resulting necessary conditions are fulfilled by a list $(\mathbf{f}_{\hat{u}}^{(\kappa)},\mathbf{f}_{\bar{u}}^{(\kappa)})$ verifying (13), (14), and the system

$$\begin{cases}\mathbf{S}_{x\hat{u}}^T\mathbf{W}\mathbf{S}_{x\hat{u}}\mathbf{f}_{\hat{u}}^{(\kappa)} = \mathbf{S}_{x\hat{u}}^T\mathbf{W}\left(\mathbf{w} - \mathbf{u}_x^{(\theta+\gamma)}\right) - \mathbf{S}_{x\hat{u}}^T\mathbf{W}\mathbf{S}_{x\bar{u}}\mathbf{f}_{\bar{u}}^{(\kappa)}\\ \left[\mathbf{S}_{x\bar{u}}^T\mathbf{W}\left(\mathbf{w} - \mathbf{u}_x^{(\theta+\gamma)}\right) - \right.\\ \left.\mathbf{S}_{x\bar{u}}^T\mathbf{W}\left(\mathbf{S}_{x\hat{u}}\mathbf{f}_{\hat{u}}^{(\kappa)} + \mathbf{S}_{x\bar{u}}\mathbf{f}_{\bar{u}}^{(\kappa)}\right)\right]\cdot\mathrm{sgn}(\mathbf{f}_{\bar{u}}) \ge 0\,,\end{cases} \tag{17}$$

where 'sgn' denotes the signature of the vector.

Solutions of (17) can be searched for a given $\mathbf{u}_x^{(\theta+\gamma)}$. Again, a control of this type can rarely be applied, as a direct measure of $\mathbf{u}_x^{(\theta+\gamma)}$ is never available (as the control affects the motion) and a computation of this array based upon a numerical model of the structure fed with data recorded from the external excitation would probably not be reliable enough (case of feedforward algorithms).

The system (17) was solved to check the feasibility of a control of the vault in terms of the order of magnitude of the needed control forces and to test, comparing results, the performance of the feedback loops presented in the next paragraph. Solutions were sought for $\mathbf{w} = \mathbf{u}_x^{(\gamma)}$ and $\mathbf{W}$ the identity or a diagonal matrix (Brocato *et al.* 2001b).

4.2.2 Instantaneous optimal control

A different strategy is required to make use of data resulting from a monitoring of $\mathbf{u}_x$ (feedback algorithm). Notice that such measures of displacements of the degrees of freedom which need be controlled may not be always feasible. In our case we assume that a sufficient number of points of measure of the displacements of the intrados of the vault can be monitored e.g. through optical instruments (digital cameras or laser scattering).

In the case of instantaneous optimal controls, advantage is taken of the fact that a change in the external excitation modifies a controlled, optimal, condition and thus only the corresponding optimal changes in the actuating forces need be computed. An incremental formulation of the problem will be considered here.

Let us assume that the task is that of minimizing at all times (time is now just a parameter ordering events) the absolute value of displacements of type x ($\mathbf{K}$ depends in general on the process),

$$\begin{cases}\mathbf{K}\mathbf{u} + \mathbf{f} = 0\,,\\ \min\limits_{\mathbf{f}_u^{(\kappa)}}\left\{|u_{xi}| \quad | \quad |f_{ui}| \le \bar{f}\;\forall i\right\}\end{cases} \tag{18}$$

(plus boundary conditions). Call $\tilde{\mathbf{K}}$ the tangential stiffness matrix; all previous definitions of $\mathbf{C}$, $\mathbf{\Phi}$, $\mathbf{S}_{xu}$ should be repeated with $\tilde{\mathbf{K}}$ replacing $\mathbf{K}$ to define the corresponding tangential matrices $\tilde{\mathbf{C}}$, $\tilde{\mathbf{\Phi}}$, $\tilde{\mathbf{S}}_{xu}$.

If the present displacements are $\mathbf{u}$, the thermal loads increase of $\Delta\mathbf{f}^{(\theta)}$, the answer of the control systems in terms of an increase of control forces $\Delta\mathbf{f}_u^{(\kappa)}$ will be the solution of

$$\begin{cases}\tilde{\mathbf{K}}\mathbf{v}^{(\theta)} + \Delta\mathbf{f}^{(\theta)} = 0\,,\\ \tilde{\mathbf{K}}\mathbf{v}^{(\kappa)} + \Delta\mathbf{f}^{(\kappa)} = 0\,,\\ \min\limits_{\Delta\mathbf{f}_u^{(\kappa)}}\left\{\left|u_{xi} + v_{x_i}^{(\theta)} + v_{x_i}^{(\kappa)}\right| \quad | \quad |f_{ui}| \le \bar{f}\;\forall i\right\}\,.\end{cases} \tag{19}$$

The increment of displacement due to the control forces can be searched solving the condensed system

$$\begin{cases}\tilde{\mathbf{C}}\mathbf{v}_u^{(\kappa)} + \Delta\mathbf{f}_u^{(\kappa)} = 0\,,\\ \mathbf{v}_x^{(\kappa)} = -\tilde{\mathbf{\Phi}}_{xu}\mathbf{v}_u^{(\kappa)}\,,\\ \mathbf{v}_s^{(\kappa)} = -\tilde{\mathbf{\Phi}}_{su}\mathbf{v}_u^{(\kappa)}\,.\end{cases} \tag{20}$$

Formally the control problem is reduced to the search of

$$\min_{\Delta\mathbf{f}_u^{(\kappa)}}\left\{\left|\mathbf{u}_x + \mathbf{v}_x^{(\theta)} + \tilde{\mathbf{S}}_{xu}\Delta\mathbf{f}_u^{(\kappa)}\right| \quad | \quad |f_{ui}| \le \bar{f}\;\forall i\right\}\,, \tag{21}$$

where $\mathbf{v}^{(\theta)}$ is the solution of

$$\tilde{\mathbf{K}}\mathbf{v}^{(\theta)} + \Delta\mathbf{f}^{(\theta)} = 0\,. \tag{22}$$

In practical circumstances of feedback loops, the matrix $\tilde{\mathbf{S}}_{xu}$ and the displacements $\mathbf{u}_x + \mathbf{v}_x^{(\theta)}$ can be evaluated by direct measure; $\tilde{\mathbf{S}}_{xu}$ is the tangent compliance correlation matrix giving generalized displacements of type x corresponding to unit forces of type u; its n-th column is the list of $\mathbf{u}_x^{(\tau)}$ displacements corresponding to application of test forces $f_{u_n}^{(\tau)} = 1$, all other entries of $\mathbf{f}_u^{(\tau)}$ being null. Sampling can be automatically performed on the structure when needed (e.g. at each relevant change of measured displacements) using the actuators to apply the test forces. The controlled degrees of freedom x should be supplied with sensors to monitor the actual state of the structure.

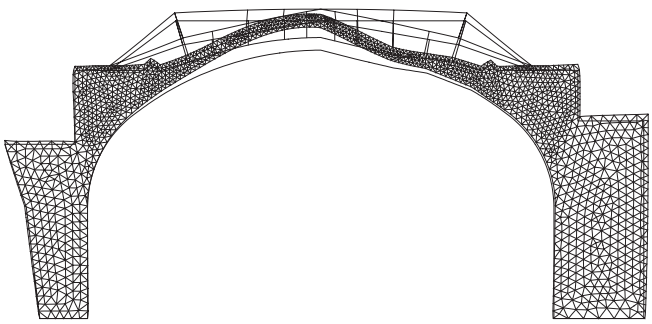

Fig. 2 Plot of the uncontrolled deformation of the structure under extreme summer conditions (the contour line represents the undeformed structure; the amplification factor of displacements is 150)

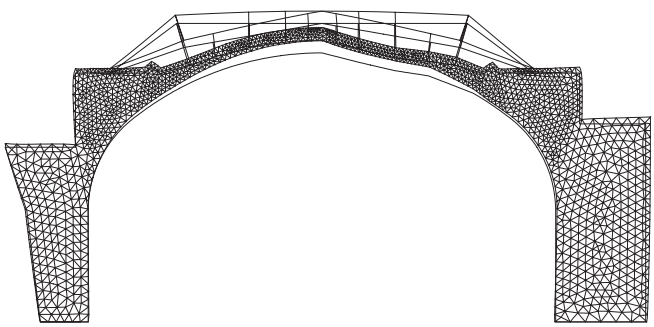

Fig. 3 Plot as in Fig. 2, but for the controlled deformation

The analysis of our results shows the feasibility and efficacy of the proposed control system.

4.3 Implementation of the algorithm

The control algorithm described in Sect. 4.2.2 was implemented numerically. Computations performed through the model described in Sect. 3 were necessary to simulate the structure.

For a closed loop control the code performs the following steps:

1. simulate a sample $\mathbf{u}_x$,
2. simulate an evaluation of $\mathbf{S}_{xu}$, i.e. do for all i:
   (a) $f_{u_i}^{(\tau i)} = \delta_{ij}$,
   (b) simulate application of $\mathbf{f}_u^{(\tau i)}$ on the structure,
   (c) simulate measurement of $\mathrm{col}_i(\mathbf{S}_{xu}) = \mathbf{u}_x^{(\tau i)}$,
3. solve minimization (21) with a constrained linear least square algorithm,
4. simulate application of the increment $\Delta\mathbf{f}_u^{(\kappa)}$ on the structure,
5. simulate measurement of $\mathbf{u}_x$,
6. compare the present and previous entries of $\mathbf{u}_x$ and:
   (a) go to line 1 if they are close enough,
   (b) go to line 3 if there is a sensible difference,
   (c) go to line 2 if there is a large difference.

If an open loop control method is sought the algorithm is simpler (but care must be taken for the accuracy of predictions needed at step 2):

1. simulate a sample of temperature,
2. evaluate $\mathbf{u}_x$,
3. simulate an evaluation of $\mathbf{S}_{xu}$ (see the corresponding closed loop steps),
4. solve (21) with a constrained linear least square algorithm,
5. simulate application of the increment $\Delta\mathbf{f}_u^{(\kappa)}$ on the structure,
6. go to line 1.

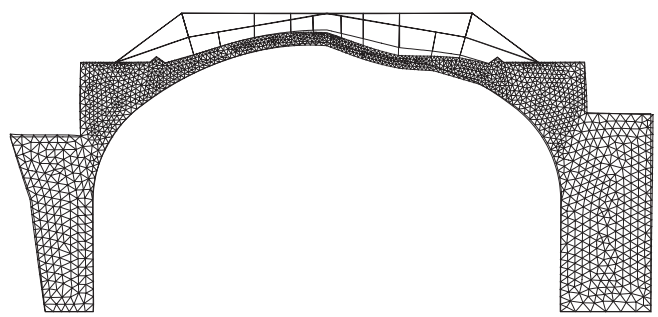

Fig. 4 Plot of the uncontrolled deformation of the structure under extreme winter conditions (the contour line represents the undeformed structure; the amplification factor of displacements is 150)

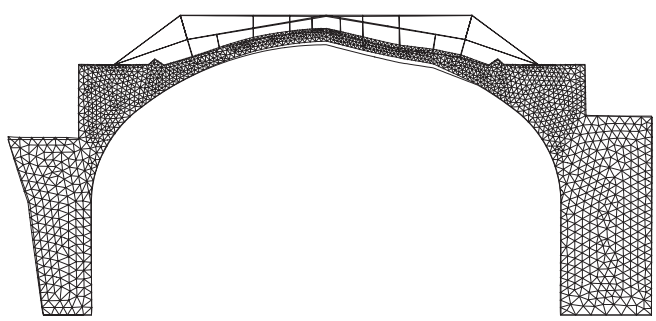

Fig. 5 Plot as in Fig. 4, but for the controlled deformation

5
Results and conclusions

Numerical results obtained for the first optimal direct control strategy presented in Sect. 4.2.1 shown that a dramatic reduction of the vertical displacements of the controlled points can be achieved with control forces the absolute value of which remains always below 45 kN (Brocato *et al.* 2001b). These results supported the feasibility of the control method and suggested to investigate on more engineering applicable strategies, such as the closed loop control algorithm presented in Sect. 4.2.2.

Dealing with the strategy given in Sect. 4.2.2, two different targets of the control were considered, corresponding to different sets of points x:

- 10 points of the extrados of the vault on which the motion controllers act (u and x degrees of freedom coincide; target 1), and
- 10 points of the intrados where the permanent deformations are larger (target 2).

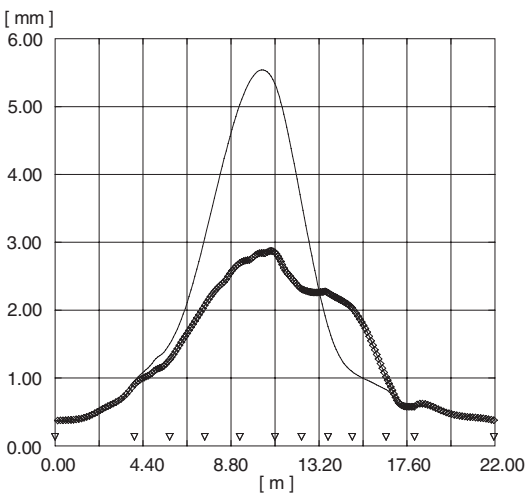

Fig. 6 Plot of the displacements of the intrados of the vault vs. mesh nodes under extreme summer conditions

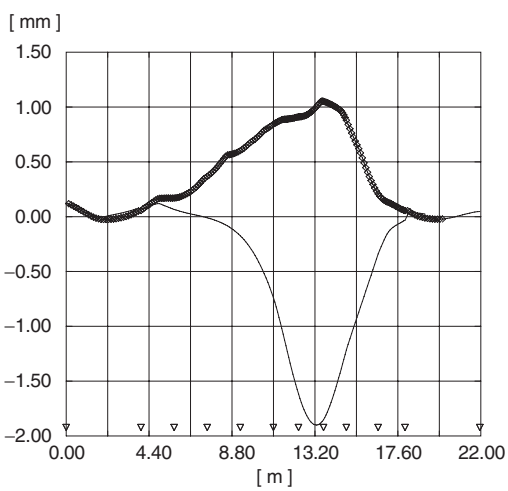

Fig. 7 Plot as in Fig. 6, but under extreme winter conditions

Correspondingly two different monitoring conditions for feedback must be implemented.

Numerical results have been obtained for a simulated history of thermal loads. If target 1 is pursued, open and closed loop results are practically equivalent for extreme winter conditions, while they show little difference for extreme wummer conditions (Brocato *et al.* 2001a). Considering a continuous variation of temperature from winter to summer conditions it was also shown that the closed loop algorithm leads to a significative reduction of the vertical displacements of the vault (Brocato *et al.* 2001a).

Although the former results proved the feedback control algorithm to be rather proficient in terms of its performance index, issues related to structural side effects of the control were left open. To answer to these questions a numerical analysis of the structure was performed under the loading conditions given by the feedback control.

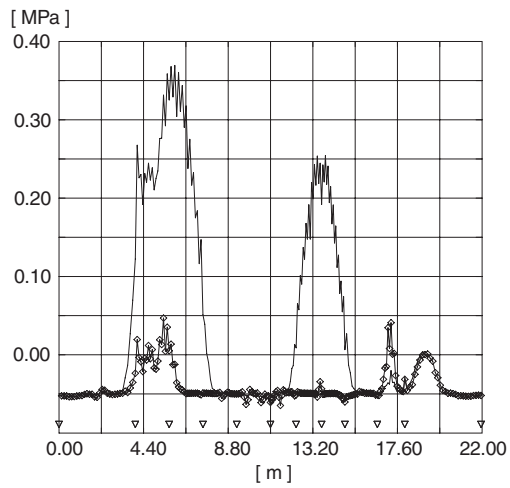

Fig. 8 Plot of the maximum (mainly tensile) principal stress along the intrados of the vault under extreme Summer conditions in the uncontrolled (plain line) and controlled (diamonds) case

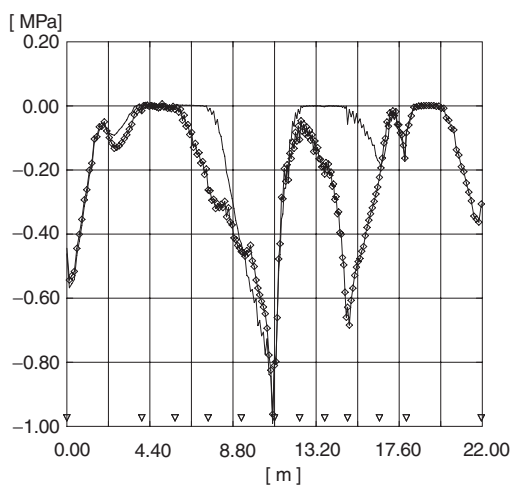

Fig. 9 Plot as in Fig. 8, but for the minimum (mainly compressive) principal stress

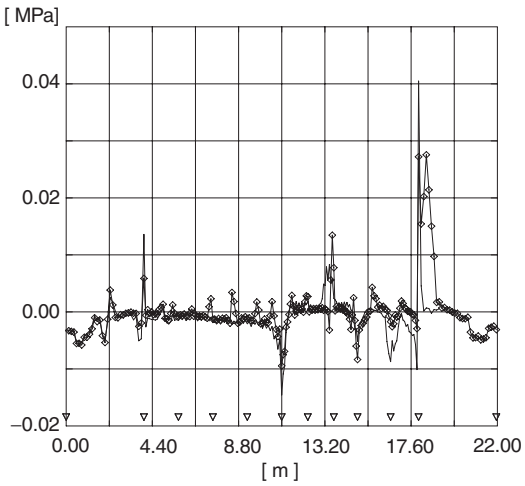

Fig. 10 Plot as in Fig. 8, but under extreme winter conditions

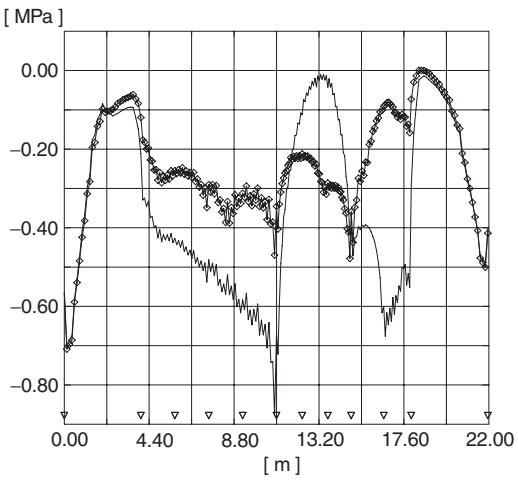

Fig. 11 Plot as in Fig. 9, but under extreme winter conditions

The following results are given for both extreme summer and winter thermal conditions (results for summer are given first).

- Plot of a sketch of the undeformed structure with a superposed deformed mesh resulting from computations in both the uncontrolled and controlled case (Figs. 2, 3, 4 and 5).
- Superposed plots of vertical displacements vs. mesh nodes at the intrados in the two quoted cases (Figs. 6 and 7).
- Plots of the principal stresses along the intrados of the vault in the uncontrolled and controlled cases (Figs. 8, 9, 10 and 11).

Acknowledgements The work reported herein was carried out during the research school "Structural problems and control methods for natural and cultural wealth conservation" funded by the European Social Fund and the *Provincia Regionale di Messina*, and within the project *"Modelli Matematici per la Scienza dei Materiali"* of the Italian *Ministero dell'Università e della Ricerca Scientifica e Tecnologica*.

Finite element computations were performed through the code CASTEM 2000, by courtesy of *Commissariat pour l'Energie Atomique*, Saclay (France).

The authors thanks *Ente Palazzo Ducale* and *Soprintendenza ai Beni Culturali* of Genoa (Italy) for information provided by them.

References

Brocato, M.; De Domenico, A.; Zanghì, F. 2001a: Feedback control of a masonry vault. In: Brebbia, C.A. (ed.) *Structural studies, repairs and maintenance of historical buildings VII*, pp. 371–379. Southampton: WIT Press

Brocato, M.; De Domenico, A.; Zanghì, F. 2001b: Numerical evaluation of the synthesis control function for an actively reinforced masonry vault. In *Proc. 1-st Albert Caquot Int. Conf. Modelling and Simulation in Civil Engineering: from Practice to Theory* (held in Paris, 3–5 Oct.), p. 84. Paris: Presses de l'Ecole Nationale des Ponts et Chaussées

Croci, G. 1986: *Il Palazzo Ducale di Genova*. Genova: Ente Palazzo Ducale

Osti, C.; Oliva, C.; Perego, F.; Spalla, G.; Croci, G.; Cerone, M. 1988: *Palazzo Ducale*. Rome: Editer

Speciale, M.P.; Brocato, M. 2001: Layered materials. *Tech. Rep. Istituto di Elaborazione della Informazione, Consiglio Nazionale delle Ricerche, Pisa. IEI-2001-TR-06*

U.S. Panel on Structural Control Research 1997: Structural control: past, present, and future. *J. Eng. Mech.* **123**, Special Issue, 897–971

View publication stats